0026-895X/06/6901-119–129$20.00
MOLECULAR PHARMACOLOGY
Copyright © 2006 The American Society for Pharmacology and Experimental Therapeutics
Mol Pharmacol 69:119–129, 2006

Vol. 69, No. 1
16840/3070904
Printed in U.S.A.

Revisiting the Postulated "Unitary Glutamate Receptor": Electrophysiological and Pharmacological Analysis in Two Heterologous Expression Systems Fails to Detect Evidence for Its Existence

Carsten Schmidt, Markus Werner, and Michael Hollmann

Department of Biochemistry I-Receptor Biochemistry, Ruhr University Bochum, Bochum, Germany

Received July 15, 2005; accepted October 7, 2005

ABSTRACT

Several years ago evidence for a so-called "unitary glutamate receptor" was published. This unique type of glutamate receptor was reported to be activated by the traditional agonists of all three major glutamate receptor subfamilies [i.e., α-amino-3-hydroxy-5-methyl-4-isoxazole propionate (AMPA), kainate, and *N*-methyl-D-aspartate (NMDA)] in a glycine-dependent as well as magnesium-blockable manner and was reported to consist of an NR1 subunit coexpressed with the kainate binding protein (KBP) from *Xenopus laevis*, *Xen*U1. To re-examine the existence of such a receptor, we cloned two splice variants of the *X. laevis* NMDA receptor subunit NR1, *Xen*NR1-4a and *Xen*NR1-4b, and expressed them in *X. laevis* oocytes as well as in human embryonic kidney (HEK) 293 cells, either alone or with the *X. laevis* KBP subunit *Xen*U1. In addition, we coexpressed *Xen*U1 separately with all eight splice variants of the rat NR1 subunit. In no case did we see evidence of a unitary glutamate receptor pharmacology. In HEK293 cells, we did not get receptor response unless an NR2 subunit was coexpressed. In *X. laevis* oocytes, we did observe responses to glutamate/glycine as well as small responses to glycine alone, but these were independent of coexpressed *Xen*U1. Neither AMPA nor kainate ever elicited significant responses. Because we verified that *Xen*U1 is expressed and inserted into the plasma membrane of HEK293 cells, we conclude that *Xen*U1 and NR1 do not form the postulated unitary glutamate receptor. Furthermore, successful amplification of a fragment of a *X. laevis* NR2 subunit indicates that *X. laevis* uses NR2 subunits and not *Xen*U1 to form heteromeric complexes with NR1.

Ionotropic glutamate receptors (iGluRs) constitute by far the most abundant excitatory neurotransmitter receptor system in the central nervous system (CNS). Therefore, it was perhaps not surprising that long before the cloning of the first glutamate receptor subunit, GluR1 (Hollmann et al., 1989), a subdivision of the iGluRs into the functionally distinct groups of NMDA and non-NMDA receptors had been proposed based on pharmacological evidence (Watkins and Evans, 1981; Mayer and Westbrook, 1987). Thereafter, additional pharmacologically distinguishable receptor subtypes were identified, which eventually were confirmed at the molecular level when recombinantly expressed cDNAs allowed specific functional analysis of their electrophysiological and pharmacological properties (for review, see Hollmann and Heinemann, 1994; Dingledine et al., 1999; Hollmann, 1999). In addition to the 16 subunits classified as components of either AMPA receptors (GluR1 to GluR4), KA receptors (GluR5 to GluR7, KA1, and KA2) or NMDA receptors (NR1, NR2A to NR2D, NR3A, and NR3B), several additional subunits were identified, which did not assemble into functional ion channels. These included the δ subunits δ1 and δ2 and the KBPs, which so far have been found exclusively in non-mammalian vertebrates such as amphibians, birds, and fish (Henley, 1994; Wo and Oswald, 1995; Hollmann, 1999), with up to two different subunits identified in any one species (goldfish; Wo and Oswald, 1994). The KBPs have the distinction of being only half the size of all other iGluRs (~50 kDa), which sets them aside as a structurally distinct group among the iGluRs.

This work was supported by the Deutsche Forschungsgemeinschaft Graduate School GRK 736.
Article, publication date, and citation information can be found at http://molpharm.aspetjournals.org.
doi:10.1124/mol.105.016840.

ABBREVIATIONS: iGluR, ionotropic glutamate receptor; CNS, central nervous system; NMDA, *N*-methyl-D-aspartate; AMPA, α-amino-3-hydroxy-5-methyl-4-isoxazole propionate; KA, kainate; KBP, kainate binding protein; HEK, human embryonic kidney; PCR, polymerase chain reaction; RT-PCR, reverse transcription-polymerase chain reaction; bp, base pair(s); EGFP, enhanced green fluorescent protein; NFR, normal frog Ringer; I/V, current-voltage; MK-801, (−)-5-methyl-10,11-dihydro-5*H*-dibenzo[*a*,*d*]cyclohepten-5,10-imine maleate; DNQX, 6,7-dinitrochinoxaline-2,3-dione.

However, several independent studies questioned the commonly used functional classification of the iGluRs and reported, for example, the existence of receptor complexes that united pharmacological properties of NMDA and non-NMDA receptors (Jahr and Stevens, 1987). These findings, which were largely based on pharmacological experiments, were not confirmed at the molecular level until Soloviev et al. (1996) described a "unitary glutamate receptor" with unusual pharmacological properties. This receptor, a heteromeric complex consisting of the *Xenopus laevis* NMDA receptor splice variant *Xen*NR1-4b and the *X. laevis* kainate binding protein *Xen*U1, responded equally to AMPA, KA, and NMDA. Even more unusual, all three agonist responses were dependent on glycine as a coagonist, and all three were blocked in a voltage-dependent manner by extracellular magnesium. Soloviev et al. (1996) extensively investigated this unitary glutamate receptor by electrophysiological analysis in HEK293 cells, coimmunoprecipitation studies, and ligand binding studies. The latter experiments also indicated that *Xen*U1 did not only form a unitary glutamate receptor complex with *X. laevis* NR1 but also with mammalian NR1 subunits (Soloviev et al., 1996). This finding and the observation that *Xen*U1 is expressed in oocytes endogenously (Soloviev and Barnard, 1997) were used to explain the appearance of functional NMDA-gated ion channels when NR1 subunits are expressed in *X. laevis* oocytes in the absence of NR2 subunits (Moriyoshi et al., 1991; Hollmann et al., 1993).

Our group had cloned *Xen*U1 several years ago for an ion pore transplantation study in which we showed that the ion pore domains of all KBPs can be transplanted into other iGluRs (e.g., the KA receptor subunit GluR6) without loss of ion channel function (Villmann et al., 1997). At the time, we also coexpressed *Xen*U1 with the rat NR1 subunit but failed to observe unusual pharmacological properties. Because the original observation of the unitary glutamate receptor had been made with the *X. laevis* version of NR1, *Xen*NR1, this left the formal possibility of a species-specific difference in the formation of the unitary glutamate receptor, a possibility that we could not rule out for lack of the *Xen*NR1 cDNA. After a recent study from Steve Heinemann's group (Green et al., 2002) re-examined the interaction of *Xen*U1 and rat NR1-1a and similarly failed to find indications for functional or structural interactions, we decided to take up the issue again. We therefore cloned two splice variants of *Xen*NR1 from *X. laevis* cDNA and analyzed their functional properties in two heterologous expression systems, *X. laevis* oocytes as well as HEK293 cells, in each case with and without coexpressed *Xen*U1. In addition, we used all eight known functional splice variants of the rat NR1 subunit (Hollmann et al., 1993) to investigate a possible splice variant-dependent functional interaction with *Xen*U1.

Materials and Methods

Isolation of the *Xen*NR1-4a cDNA and Construction of the *Xen*NR1-4b and *Xen*NR1-4b(E166G) cDNAs. For the cloning of *X. laevis* glutamate receptor subunits, three degenerate oligonucleotides were designed as PCR primers based on a sequence alignment of GluR1 (GenBank accession no. X17184), KA1 (U08257), GluR6 (Z11548), NR1-1a (U08261), and *Xen*NR1 (X94081). These primers, 5′-GGCTWYTGYRTSGACCTG-3′ (alternatively, 5′-TGGAAYGGMATGRTKGGMG-3′) and 5′-GAARGCWGCCARGTTRGC-3′ (with K = G/T, M = A/C, R= A/G, S = G/C, Y = C/T, and W = A/T), were used in an RT-PCR of RNA extracted from adult female *X. laevis* brain as template. A 594-bp fragment of *Xen*NR1 (Soloviev et al., 1996) beginning at position +1425 was amplified. The PCR product was radiolabeled with [α-^{32}P]dCTP using HexaLabel DNA labeling kit (MBI Fermentas, St. Leon-Rot, Germany) and used as a probe to screen 5×10^5 plaques of a *X. laevis* embryo cDNA library (Stratagene, La Jolla, CA) at high-stringency conditions (125 mM NaCl, 7.5 mM Tris-HCl, pH 7.4, 0.5 mM EDTA, 5× Denhardt's solution, 0.5% SDS, and 100 μg/ml salmon sperm DNA at 65°C). The nylon filters (Roche Diagnostics, Mannheim, Germany) were washed in washing buffer (50 mM NaCl, 3 mM Tris-HCl, pH 7.4, 0.2 mM EDTA, and 0.1% SDS) at 65°C. One clone was selected for further study and was plaque-purified, rescued as pBluescript plasmid, and analyzed by restriction endonuclease digestion and sequencing. We identified the isolated clone as a full-length NMDA receptor subunit from *X. laevis* lacking a 63-bp sequence (=exon 5 in rat) in the region encoding for the N-terminal domain compared with the published *Xen*NR1 sequence. Further differences to *Xen*NR1 are six single base deviations (positions 120, 557, 756, 2130, 2202, and 2223 of the *Xen*NR1 coding region) of which five do not alter the encoded amino acid. Only the deviation at position 557 alters the amino acid sequence of the encoded protein by replacing glycine 166 of the mature protein by glutamate. Because of the homology of the cloned *X. laevis* glutamate receptor subunit compared with the NR1-4a splice variant from rat, we called the cloned subunit *Xen*NR1-4a. The *Xen*NR1-4a cDNA sequence has been deposited in GenBank (accession no. DQ066918).

The 63-bp sequence that *Xen*NR1-4a is missing compared with the published *Xen*NR1 sequence (which is the *Xen*NR1-4b splice variant) was confirmed to be expressed in frog brain by performing an RT-PCR on adult female *X. laevis* brain RNA using primers flanking the 63-bp sequence (5′-ATGCCATCCAGATGGCTCTATCTGT-3′ and 5′-GAGGAGTATAACTCTGGCTTCCAGT-3′). Fragments of interest were isolated, subcloned into the EcoRV site of pSGEM, and analyzed by sequencing.

For the introduction of the 63-bp sequence into *Xen*NR1-4a, two overlapping tail primers were synthesized: 5′-CCTCGACCAACTTTCCTATGACAACAAGCGTGGACCCAAGGCAGACAAAGTCCTGCAGTT-3′ and 5′-AGGAAAGTTGGTCGAGGTTCTCATAGTTCCTTTTTTTACCCTTGGACTCTTTCTCCTCTA-3′. These tail primers were used together with the oligonucleotides 5′-GCTTGGAGCTGAGAGCACCCA-3′ and 5′-CATATACAAAAGGTTCTTGGTGGA-3′ as primers in an overlap extension PCR. The resulting 1354-bp PCR product and *Xen*NR1-4a were digested with BglII and Bpu10I and ligated to produce *Xen*NR1-4b.

Because our *Xen*NR1-4b contained a glutamate at position 166 instead of a glycine reported for the cDNA clone of Soloviev et al. (1996), we introduced a glycine by PCR-mediated mutagenesis with the mutagenesis primers 5′-TTACTCTTGGACTCTTTCCCCTCTAACAGGGTCTC-3′ and 5′-TGGAGACCCTGTTAGAGGGGAAAGAGTCCAAGAGT-3′. The resulting 1354-bp PCR product, which contained the E166G mutation, and *Xen*NR1-4b were digested with BglII and Bpu10I and ligated to produce *Xen*NR1-4b(E166G).

To screen for C-terminally alternatively spliced forms of *X. laevis* NR1, we performed several RT-PCRs. First, we used oligonucleotides flanking the putative alternatively spliced regions (5′-GAACTCAGCACTATGTACAGACACA-3′ and 5′-CCAGTCATTAGCCGTCAGTACA-3′). Second, we used a sense primer lying upstream of the putative splice sites (5′-GAACTCAGCACTATGTACAGACACA-3′) and antisense primers located in the exons 21 (5′-TCTCTTGAAGCTGGAGGCCA-3′) and 22 (5′-TAACGGGCCGCCTTGTCTGT-3′) of *Rattus norvegicus*.

For electrophysiological investigation of the isolated *Xen*NR1-4 subunits in *X. laevis* oocytes and HEK293 cells, the cDNAs were subcloned into the expression vectors pSGEM-KS and pcDNA3 (Invitrogen, Karlsruhe, Germany), respectively.

Tagging of Receptor Subunits. For Western blot analysis, *Xen*U1 (GenBank accession no. DQ073428, isolated in our laboratory previously; Villmann et al., 1997) was C-terminally tagged with a

myc epitope-encoding sequence and a polyhistidine tag. To create *Xen*U1-myc-His, the complete *Xen*U1 coding region was amplified by PCR using the primers 5′-CCCAGCTTGCTTGTTCTTT-3′ and 5′-AGAATCCTCGAGTGATTTCACACTGTCCACTGCT-3′, thus replacing the native stop codon by an XhoI restriction site. The PCR product was digested with EcoRV and XhoI and ligated into the EcoRV/XhoI-cut pcDNA4/TO/myc-His vector (Invitrogen).

For the analysis of the subcellular localization of *X. laevis* NR1 receptor subunits and *Xen*U1 in HEK293 cells by confocal microscopy, the subunits were C-terminally tagged with EGFP and DsRed2, respectively. The cDNAs of the *Xen*NR1 subunits were subcloned into the XhoI and SacII restriction sites of pEGFP-N1 (BD Biosciences Clontech, Palo Alto, CA). The stop codon was deleted by performing a PCR using the primers 5′-GAACTCAGCACTATGTACAGACACA-3′ and 5′-TGATGGACCGGTGCGACCACAGTGCTAACAGAAG-3′, after restriction digest of the PCR product (578 bp) with AgeI and ligation of the fragment into the AgeI-cut *Xen*NR1-4(a/b)/pEGFP-N1, producing *Xen*NR1-4a-EGFP and *Xen*NR1-4b-EGFP. To create *Xen*U1-DsRed2, the *Xen*U1 cDNA was isolated by a restriction digest with XbaI and XhoI and ligated into the NheI/XhoI-cut pDsRed2-N1 vector (BD Biosciences Clontech). The *Xen*U1 C terminus was amplified by PCR using the primers 5′-GATGAACTTCTTGTGAAATCA-3′ and 5′-CAGAATGGGCCCATGATTTCACACTGTCCACTG-3′. The PCR product (523 bp) was digested with ApaI and ligated into ApaI-cut *Xen*U1/pDsRed2-N1.

cRNA Synthesis. cRNA synthesis was done as described previously (Hollmann et al., 1994). In brief, template DNA was linearized with NheI. cRNA was synthesized from 1 μg of linearized DNA using an in vitro transcription kit (MBI Fermentas) with a modified protocol that uses 800 μM GpppG (MBI Fermentas) for capping and an extended reaction time of 3 h with T7 polymerase. Trace labeling was performed with [α-^{32}P]UTP to allow calculation of yields and evaluation of transcript quality by agarose gel electrophoresis.

Electrophysiological Studies in *X. laevis* Oocytes. Frog oocytes of stages V or VI were surgically removed from the ovaries of *X. laevis* (Nasco, Fort Atkinson, WI) anesthetized with 3-amino-benzoic acid ethylester (1.5 g/l; Sigma, Taufkirchen, Germany). Lumps of ~20 oocytes were incubated with 784 U/ml (4 mg/ml) collagenase type I (Worthington Biochemicals, Freehold, NJ) for 1.5 h in Ca^{2+}-free Barth's solution (88 mM NaCl, 1.1 mM KCl, 2.4 mM $NaHCO_3$, 0.8 mM $MgSO_4$, and 15 mM HEPES, pH adjusted to 7.6 with NaOH) with slow agitation to remove the follicular cell layer and then washed extensively with Barth's solution [88 mM NaCl, 1.1 mM KCl, 2.4 mM $NaHCO_3$, 0.3 mM $Ca(NO)_3$, 0.4 mM $CaCl_2$, 0.8 mM $MgSO_4$, and 15 mM HEPES, pH adjusted to 7.6 with NaOH)]. Oocytes were maintained in Barth's solution with 100 μg/ml gentamycin, 40 μg/ml streptomycin, and 63 μg/ml penicillin added. Twenty-four hours later, oocytes were injected with a total of 10 ng of cRNA for single expressions and with 20 ng for coexpressions (10 ng each) using a nanoliter injector (WPI, Sarasota, FL). Four to 5 days after injection, oocytes were recorded in normal frog Ringer's solution (NFR; 115 mM NaCl, 2.5 mM KCl, 1.8 mM $CaCl_2$, and 10 mM HEPES, pH adjusted to 7.2 with NaOH) under voltage clamp at −70-mV holding potential [except for current-voltage (I/V) curves], with a TurboTec 10CX amplifier (NPI Electronic GmbH, Tamm, Germany) controlled by Pulse software (HEKA, Lambrecht/Pfalz, Germany). Recording pipettes were pulled from borosilicate glass (Hilgenberg, Malsfeld, Germany) using a PIP5 pipette vertical puller (HEKA). Voltage electrodes had a resistance of 1 to 4 MΩ and were filled with 3 M KCl; current electrodes had a resistance of 0.5 to 1.5 MΩ and were filled with 3 M CsCl. Drugs were applied for 20 s by superfusion at a flow rate of ~5 ml/min. Coapplication of agonists is indicated by a slash between the agonists throughout this article (e.g., glutamate/glycine). For I/V curves, agonist was applied by constant superfusion, and a 2-s voltage ramp from −150 to +50 mV was recorded at the peak current, disregarding the initial fast spike that has been shown to represent a Ca^{2+}-activated Cl^- conductance endogenous to *X. laevis* oocytes (Leonard and Kelso, 1990). Voltage ramps recorded before and after agonist application were averaged and subtracted from I/V curves for leakage current correction. To determine EC_{50} values for glutamate and NMDA, 10 to 12 different agonist concentrations were applied to the same oocyte, and steady-state values of the evoked currents were measured. Data from each oocyte were fitted separately, and EC_{50} values obtained this way from four oocytes were averaged. For investigation of NMDA receptor-specific Mg^{2+} block, Mg^{2+}-Ringer's solution was used (115 mM NaCl, 2.5 mM KCl, 1.8 mM $MgCl_2$, and 10 mM HEPES, pH adjusted to 7.2 with NaOH).

HEK293 Cell Transfection. HEK293 cells were transfected with recombinant vector DNA using a modified calcium phosphate precipitation technique (Chen and Okayama, 1987). Exponentially growing cells in polyornithine-coated 35-mm dishes were transfected with 2 to 5 μg of DNA. For precipitation, a mixture of 2 μg of each DNA, 10 μl of $CaCl_2$ (2.5 M), and water (ad 100 μl) was incubated for 20 min at room temperature. Next, 100 μl of 2× HEPES-buffered saline [280 mM NaCl, 1.5 mM Na_2HPO_4, and 40 mM HEPES, pH adjusted to 7.1 with NaOH] was added, and the mixture was incubated for 20 min at room temperature. Then, 500 μl of cell culture medium (Dulbecco's modified Eagle's medium and 10% fetal bovine serum) was added in droplets. The whole mixture was transferred to a 35-mm dish, and the cells were incubated for 8 h at 37°C with 3% CO_2. After incubation, the cells were washed twice with 2 ml of phosphate-buffered saline before growth medium was added (for patch clamp and Western blots, minimal essential medium; for confocal microscopy, Earle's minimal essential medium). After transfection, HEK293 cells were allowed to express receptor for 48 to 96 h at 37°C with 5% CO_2.

If the transfected cells were analyzed by the patch-clamp technique, 1 μg of EGFP/pcDNA3 was added to the precipitation mixture. Thus, transfected cells could be identified by their green fluorescence when excited at 488 nm.

For Western blot analysis, 85-mm dishes were used. Therefore, the amount of all ingredients of the precipitation mixture was increased 6-fold.

Electrophysiological Studies in HEK293 Cells. Whole cell recordings were performed using a HEKA EPC-9 amplifier (HEKA) controlled by Pulse software (HEKA). Recording pipettes were pulled from borosilicate glass (GC150TL-10; Clarke Electromedical Instruments, Pangbourne, UK) using a PIP5 pipette vertical puller (HEKA). Ligand was applied using a theta glass capillary (Hilgenberg) that bathed the suspended cell in a laminar flow of solution, giving a time resolution for equilibration of 10 to 30 ms (Udgaonkar and Hess, 1987). The external buffer consisted of 140 mM NaCl, 4 mM KCl, 2 mM $CaCl_2$, and 10 mM HEPES, pH adjusted to 7.3 with NaOH; the internal buffer was 110 mM Cs gluconate, 20 mM CsCl, 4 mM NaCl, 1 mM $MgCl_2$, 0.5 mM $CaCl_2$, 5 mM EGTA, and 10 mM HEPES, pH adjusted to 7.4 with KOH. The current responses were measured at room temperature at a holding potential of −60 mV.

Subunit Expression Analysis by Western Blotting. Western blot analysis was performed on HEK293 cells transfected with *Xen*U1-myc-His DNA 40 h after transfection. Cells were washed in phosphate-buffered saline and swelling buffer [10 mM HEPES (pH adjusted to 7.9 with KOH), 1.5 mM $MgCl_2$, 10 mM KCl, and 0.5 mM dithiothreitol] and incubated on ice in swelling buffer afterward. Next, cells were homogenized using a douncer, and then 1/10 volume of stabilization buffer [300 mM HEPES (pH adjusted to 7.9 with KOH), 30 mM $MgCl_2$, and 1.4 M KCl] was added. Nuclei and crude cell fragments were removed by low-speed centrifugation (2500*g*; 1 min; 4°C). The supernatant was used in an ultracentrifugation (100,000*g*; 1 h; 4°C), and to the resulting membrane pellet urea buffer (8 M urea, 375 mM Tris-HCl, pH 6.8, and 0.1% SDS) and SDS-polyacrylamide gel electrophoresis loading buffer (25 mM Tris-HCl, pH 6.8, 6% SDS, 800 mM β-mercaptoethanol, 20% glycerol, 0.1% bromphenol blue, and 8 M urea) were added. Then, the sample was incubated in boiling water (10 min). Proteins were separated by SDS-polyacrylamide gel electrophoresis on an 8% gel and electroblotted on nitrocellulose membranes (GE Healthcare, Little Chalfont,

Buckinghamshire, UK). The nitrocellulose membranes were blocked with 4% nonfat dry milk (Gluecksklee, Muenchen, Germany) in Tris-buffered saline/Tween 20 (140 mM NaCl, 20 mM Tris-HCl, pH 7.6, and 0.1% Tween 20), and detection of proteins was carried out using mouse anti-myc (gift from B. J. Benecke, Ruhr University, Bochum, Germany) and donkey anti-mouse (Dianova, Hamburg, Germany) antibodies. Blots were developed using enhanced chemiluminescence solutions (Pierce Chemical, Rockford, IL).

Analysis of Subcellular Localization by Confocal Microscopy of Fluorescently Labeled Subunits. Confocal microscopy was performed on a Leica TCS SP2 (Leica, Mannheim, Germany) laser scanning confocal microscope using a Leica 63×, 1.3 numerical aperture, water immersion lens. HEK293 cells expressing *X. laevis* glutamate receptor subunits were plated on 35-mm glass-bottomed culture dishes and were kept in minimal essential medium with Earl's salts and 10% fetal calf serum but without phenol red (Sigma). During measurement, the dishes were preserved in a heated microscope chamber (H. Saur, Reutlingen, Germany), which adjusted the temperature to 37°C and the CO_2 percentage to 7% permanently. Colocalization studies were performed using dual excitation and emission filter sets. Specificity of labeling was established by examination of single labeled samples, and signal detection was optimized to ensure absence of signal crossover. For the analysis of the laser scanning confocal micrographs (including identification of colocalization), the Leica software was used.

Results

We initially set out to test whether coexpression of the *X. laevis* KBP *Xen*U1 with any of the eight known rat NR1 splice variants (Hollmann et al., 1993) can generate the reported unitary glutamate receptor. For electrophysiological investigation, the eight rat NR1 splice variants were expressed alone and together with *Xen*U1 in *X. laevis* oocytes. To test whether functional glutamate receptors were present, we applied glutamate (100 μM) together with the coagonist glycine (10 μM). Furthermore, we tested for the reported unique unitary glutamate receptor pharmacology by application of kainate (100 μM) or AMPA (100 μM), each with and without glycine. Because it is known that glycine applied alone can generate currents from NMDA receptors (Kleckner and Dingledine, 1988; Moriyoshi et al., 1991; Laube et al., 1993), we additionally applied glycine alone in all experiments. In all oocytes injected with NR1 with or without *Xen*U1, we found significant current responses upon application of glutamate/glycine. Some oocytes showed small currents also upon application of kainate/glycine, AMPA/glycine, or glycine alone, which were all equal in size. By contrast, we never obtained a current response upon application of kainate or AMPA alone (Table 1). We therefore conclude that these small currents were induced by glycine alone without any effect exerted by AMPA or kainate. In addition, we found no significant difference in current amplitudes between oocytes expressing NR1 alone or together with *Xen*U1. This finding was independent of the NR1 splice variant and included the NR1-4b splice variant (Fig. 1), which originally was reported to form ion channels of the unitary glutamate receptor type, at least for the *X. laevis* homolog of NR1-4b (Soloviev et al., 1996).

Although we found no evidence of a unitary glutamate receptor when we combined rat NR1 subunits with *Xen*U1, we could not rule out its existence because Soloviev et al. (1996) had used the *X. laevis* homolog of NR1-4b, *Xen*NR1-4b, in combination with *Xen*U1 when they observed the unitary glutamate receptor properties. To be able to analyze the exact same subunit combination as Soloviev et al. (1996) in their original description of the unitary glutamate receptor, we screened a cDNA library from *X. laevis* embryo for *Xen*NR1 cDNAs using as a probe a 594-bp fragment of a

TABLE 1

Steady-state currents of rat NR1 splice variants expressed alone and together with *Xen*U1

The currents given are the means ± S.E.M. The numbers of oocytes measured is given in parentheses. Note that currents smaller than 1 nA are not detectable in the *X. laevis* oocyte expression system. Values smaller than 1 nA result from averaging cells showing currents ≥1 nA with cells showing no current response upon application of the same agonist(s).

Expressed Subunit	Steady-State Current					
	Glu/Gly (100 μM/10 μM)	KA/Gly (100 μM/10 μM)	AMPA/Gly (100 μM/10 μM)	Gly (10 μM)	KA (100 μM)	AMPA (100 μM)
	nA					
NR1-1a						
+ *Xen*U1	6.6 ± 1.1 (10)	0.9 ± 0.3 (6)	0.7 ± 0.3 (6)	0.5 ± 0.2 (6)	0 (6)	0 (6)
− *Xen*U1	6.6 ± 0.6 (10)	0.2 ± 0.2 (6)	0.3 ± 0.2 (6)	0.2 ± 0.2 (6)	0 (6)	0 (6)
NR1-1b						
+ *Xen*U1	21.2 ± 2.8 (16)	0.5 ± 0.2 (6)	0.5 ± 0.2 (6)	0.4 ± 0.2 (6)	0 (6)	0 (6)
− *Xen*U1	17.2 ± 2.4 (17)	0.2 ± 0.2 (7)	0.3 ± 0.3 (7)	0.5 ± 0.4 (9)	0 (6)	0 (7)
NR1-2a						
+ *Xen*U1	12.2 ± 3.0 (6)	0 (4)	0 (4)	0 (4)	0 (4)	0 (4)
− *Xen*U1	12.0 ± 3.1 (8)	0.7 ± 0.6 (5)	0.2 ± 0.2 (5)	0.3 ± 0.3 (5)	0 (5)	0 (5)
NR1-2b						
+ *Xen*U1	7.4 ± 1.4 (10)	0.1 ± 0.1 (6)	0.2 ± 0.2 (6)	0.1 ± 0.1 (7)	0 (6)	0 (6)
− *Xen*U1	6.7 ± 0.8 (11)	0 (6)	0 (6)	0 (6)	0 (6)	0 (6)
NR1-3a						
+ *Xen*U1	67.8 ± 9.9 (8)	1.4 ± 0.4 (6)	1.6 ± 0.5 (6)	1.4 ± 0.5 (6)	0 (6)	0 (6)
− *Xen*U1	81.4 ± 7.4 (10)	2.4 ± 0.6 (6)	2.5 ± 0.9 (6)	2.6 ± 0.7 (6)	0 (6)	0 (6)
NR1-3b						
+ *Xen*U1	102.7 ± 23.9 (9)	0.8 ± 0.5 (6)	1.4 ± 1.0 (6)	1.5 ± 1.0 (6)	0 (6)	0 (6)
− *Xen*U1	134.9 ± 26.5 (13)	3.0 ± 1.9 (6)	2.4 ± 1.2 (6)	2.6 ± 1.4 (6)	0 (6)	0 (6)
NR1-4a						
+ *Xen*U1	10.2 ± 1.7 (8)	1.2 ± 0.6 (7)	0.9 ± 0.5 (7)	1.0 ± 0.5 (7)	0 (6)	0 (6)
− *Xen*U1	8.9 ± 1.1 (8)	0 (6)	0 (6)	0 (6)	0 (6)	0 (6)
NR1-4b						
+ *Xen*U1	22.0 ± 1.6 (9)	0.5 ± 0.4 (6)	0.4 ± 0.4 (6)	0.4 ± 0.3 (6)	0 (6)	0 (6)
− *Xen*U1	19.9 ± 5.5 (11)	0 (6)	0 (6)	0 (6)	0 (6)	0 (6)

X. laevis NR1 subunit amplified by PCR from *X. laevis* brain reverse-transcribed total RNA. One clone was identified corresponding to a full-length *X. laevis* NMDA receptor cDNA. The cDNA lacked a 63-nucleotide sequence in the N-terminal domain compared with the published *Xen*NR1; additionally, six nucleotides differed. Five of these differences did not alter the encoded amino acids (see *Materials and Methods*), whereas one alternate nucleotide replaced glycine 166 of the mature protein reported by Soloviev et al. (1996) by glutamate. Sequence comparison with the rat NR1 splice variants showed our clone to be the *X. laevis* homolog of the rat NR1-4a subunit, *Xen*NR1-4a. To obtain the *X. laevis* NR1 subunit *Xen*NR1-4b, we introduced the missing 63-bp sequence (=exon 5 in rat), which is characteristic for b splice variants (Hollmann et al., 1993), by overlap extension PCR. In addition, we amplified the sequence around the *X. laevis* exon 5 homolog by RT-PCR from *X. laevis* brain mRNA and obtained two specific bands (455 and 518 bp), which prove that a and b splice variants were expressed in adult female *X. laevis* brain. The fact that the 455-bp band was much stronger than the 518-bp band indicates that NR1 a splice variants are more common in *X. laevis* brain than b splice variants.

To check the *X. laevis* exon 5-homologous sequence, we subcloned the 518-bp fragment and analyzed it by sequencing. We found our exon 5-homologous sequence to be identical to that reported by Soloviev et al. (1996). However, we confirmed that the G166E amino acid deviation mentioned above was genuine. To screen for further *Xen*NR1 splice variants, we performed several PCRs with oligonucleotides recognizing the sequences upstream and downstream of the C-terminally spliced exons 21 and 22 known from rat NR1 (Hollmann et al., 1993), but we did not obtain evidence for the existence of more alternatively spliced forms of *Xen*NR1. By contrast, if we used a sense primer located upstream of the putative alternatively spliced exons and an antisense primer located in the sequence homologous to rat exon 21, we amplified one specific band (588 bp). Determination of the sequence of the fragment proved that a sequence homologous to rat exon 21 exists in *X. laevis* NR1 subunits. Using the same strategy with an exon 22-specific antisense primer, we obtained no specific bands. These results are evidence that in addition to NR1-4, at least the NR1–3 splice variants exist in *X. laevis*.

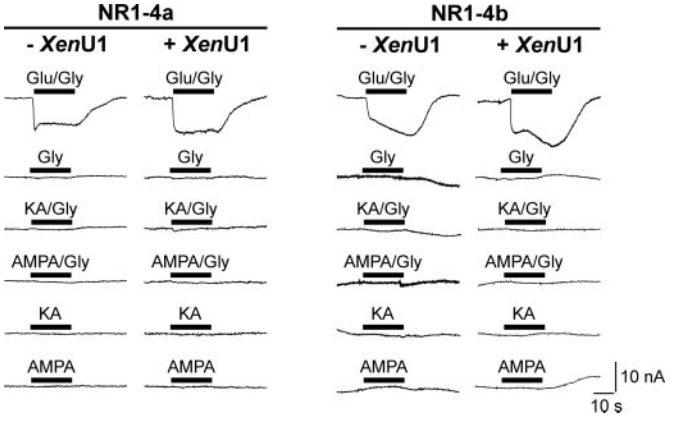

Fig. 1. Comparison of agonist-induced current responses recorded from voltage-clamped *X. laevis* oocytes injected with cRNAs of the rat NR1 splice variants NR1-4a and NR1-4b alone and together with *Xen*U1. The experimental details were as described under *Materials and Methods*. The applied agonist concentrations were 100 μM glutamate, 100 μM KA, 100 μM AMPA, and 10 μM glycine. The application of agonists is indicated by black bars.

It had been reported that the sequence encoding the N-terminal domain of *Xen*NR1 showed significant differences compared with rat NR1, and it had been suggested that these differences alter the receptor properties (Soloviev et al., 1996). Because an extensive characterization of the *X. laevis* NR1 subunit had never been reported, we tested whether the two isolated *Xen*NR1-4 splice variants are functional subunits and behave similar to mammalian NR1 subunits. We initially expressed *Xen*NR1-4a and *Xen*NR1-4b alone or with the rat NR2B subunit in *X. laevis* oocytes as well as in HEK293 cells. In oocytes, both homomerically expressed *X. laevis* NR1 subunits showed small currents upon application of 100 μM glutamate with 10 μM glycine (*Xen*NR1-4a, 3.5 $\pm$ 0.5 nA, $n = 8$; *Xen*NR1-4b, 12.0 $\pm$ 1.6 nA, $n = 5$) and 100 μM NMDA with 10 μM glycine (*Xen*NR1-4a, 1.3 $\pm$ 0.4 nA, $n = 8$; *Xen*NR1-4b, 2.6 $\pm$ 1.3 nA, $n = 5$; Fig. 2A). When we expressed the *X. laevis* NR1 splice variants together with rat NR2B, the current amplitudes were greatly increased as is found with rat NR1 subunits when coexpressed with NR2B (Ikeda et al., 1992; Kutsuwada et al., 1992; Meguro et al., 1992; Ishii et al., 1993). We obtained steady-state currents of 1100 $\pm$ 218 nA ($n = 16$) and 5917 $\pm$ 166 nA ($n = 7$) upon application of glutamate/glycine for *Xen*NR1-4a/NR2B and *Xen*NR1-4b/NR2B, respectively, and 411 $\pm$ 77 nA ($n = 16$) and 826 $\pm$ 65 nA ($n = 7$) upon application of NMDA/glycine (Fig. 2B). We then recorded dose-response curves for glutamate and NMDA, of *Xen*NR1-4a/NR2B and *Xen*NR1-4b/NR2B (Fig. 2D). We calculated EC_{50} values of 2.0 $\pm$ 0.3 μM (glutamate) and 60 $\pm$ 13 μM (NMDA) for *Xen*NR1-4a/NR2B and 2.8 $\pm$ 0.5 μM (glutamate) and 240 $\pm$ 25 μM (NMDA) for *Xen*NR1-4a/NR2B. Next, we investigated the NMDA receptor-specific glycine dependence of glutamate-induced currents known from mammalian NMDA receptors (Johnson and Ascher, 1987; Kleckner and Dingledine, 1988). We found that *Xen*NR1-4a/NR2B as well as *Xen*NR1-4b/NR2B were activated by glutamate applied alone, but the steady-state currents obtained were relatively small, 10 $\pm$ 3 nA ($n = 6$) and 94 $\pm$ 20 nA ($n = 9$), respectively. Likewise, upon application of glycine alone, small currents were obtained for *Xen*NR1-4a/NR2B (17 $\pm$ 5 nA; $n = 6$) and *Xen*NR1-4b/NR2B (211 $\pm$ 74 nA; $n = 9$). Coapplication of glutamate and glycine increased the current amplitudes for *Xen*NR1-4a/NR2B by approximately 136-fold (1361 $\pm$ 446 nA; $n = 6$) compared with glutamate-induced currents, and for *Xen*NR1-4b/NR2B by approximately 77-fold (7283 $\pm$ 658 nA; $n = 9$; Fig. 2C). Another NMDA receptor-specific property of the *X. laevis* NR1 splice variants could be shown as we analyzed the glutamate/glycine-induced current flow in the presence and absence of extracellular Mg^{2+}. We found that I/V curves recorded in Mg^{2+}-free NFR were linear for both *Xen*NR1 splice variants investigated, whereas in the presence of 1.8 mM extracellular Mg^{2+} ions the *X. laevis* NMDA receptor complexes showed rectifying I/V with no significant current flow at negative membrane potentials, but linearly increasing currents at positive membrane potentials (Fig. 2E). Further experiments showed that the receptors are not blocked by divalent cations in general but that the receptor complexes containing *X. laevis* NR1 subunits are highly permeable for Ca^{2+} ions (data not shown). In addition to the Mg^{2+} block, *X.*

laevis NMDA receptors can be blocked by MK-801. A concentration of 1 μM MK-801 was sufficient to reduce the glutamate/glycine-induced current response of *Xen*NR1-4a/NR2B and *Xen*NR1-4b/NR2B to 7 ± 2% (n = 9) and 5 ± 3% (n = 6), of the maximal currents, respectively. All these experiments demonstrate that *X. laevis* NR1 subunits are functionally equivalent to the homologous subunits from *R. norvegicus*.

After the functional analysis of the isolated *X. laevis* NR1 splice variants in *X. laevis* oocytes, we tested whether the *Xen*NR1 subunits form functional glutamate-gated ion channels also in HEK293 cells. We subcloned *Xen*NR1-4a and *Xen*NR1-4b into the expression vector pcDNA3 and transfected each subunit into HEK293 cells, alone as well as together with rat NR2B. The cells were analyzed 2 to 3 days after transfection by patch-clamp recordings using the whole cell recording mode. In cells transfected only with *Xen*NR1-4a (n = 16) or *Xen*NR1-4b (n = 15), we never detected significant current in response to the application of 100 μM glutamate plus 10 μM glycine. As expected, NR2B alone also did not form functional receptor complexes (Ikeda et al., 1992; Kutsuwada et al., 1992; Meguro et al., 1992; Monyer et al., 1992; Ishii et al., 1993). However, when we coexpressed any of the *X. laevis* NR1 splice variants and rat NR2B, approximately one-third of the patched cells showed a current response upon application of glutamate/glycine. The current amplitudes measured were 71 ± 16 pA for *Xen*NR1-4a/NR2B (n = 13) and 94 ± 29 pA for *Xen*NR1-4b/NR2B (n = 11; Fig. 3).

We then analyzed the electrophysiological properties of *Xen*NR1-4 splice variants coexpressed with *Xen*U1, the putative unitary glutamate receptor, in *X. laevis* oocytes as well as in HEK293 cells. As a control, we also expressed the *Xen*NR1 subunits alone. In oocytes, we performed applications of glutamate (100 μM), KA (100 μM), and AMPA (10 μM), each alone and together with 10 μM glycine. In addition, glycine was applied alone (Fig. 4A). We found that *Xen*NR1-4a never showed current responses to KA (with or without glycine), AMPA (with or without glycine), or glycine, neither when expressed alone nor when coexpressed with *Xen*U1. Only application of glutamate/glycine induced small currents in oocytes expressing *Xen*NR1-4a or *Xen*NR1-4a plus *Xen*U1. However, comparing the current amplitudes recorded from *Xen*NR1-4a with those obtained from *Xen*NR1-4a plus *Xen*U1, no significant differences were obtained (Table 2). When we investigated *Xen*NR1-4b, we similarly found no significant current responses upon application of KA (with or without glycine), AMPA (with or without glycine), or glycine. Exclusively glutamate was able to induce currents in the presence of glycine. When we coexpressed *Xen*NR1-4b and *Xen*U1, which is the reported subunit combination of the unitary glutamate receptor (Soloviev et al., 1996, 1998), we found in one of five oocytes tiny currents upon application of KA/glycine (1.4 nA) and AMPA/glycine (1.5 nA). However, glycine alone induced currents that were equal in size (1.0 nA), whereas application of KA or AMPA alone never induced current responses. Therefore, we conclude these currents to be induced by glycine alone, as

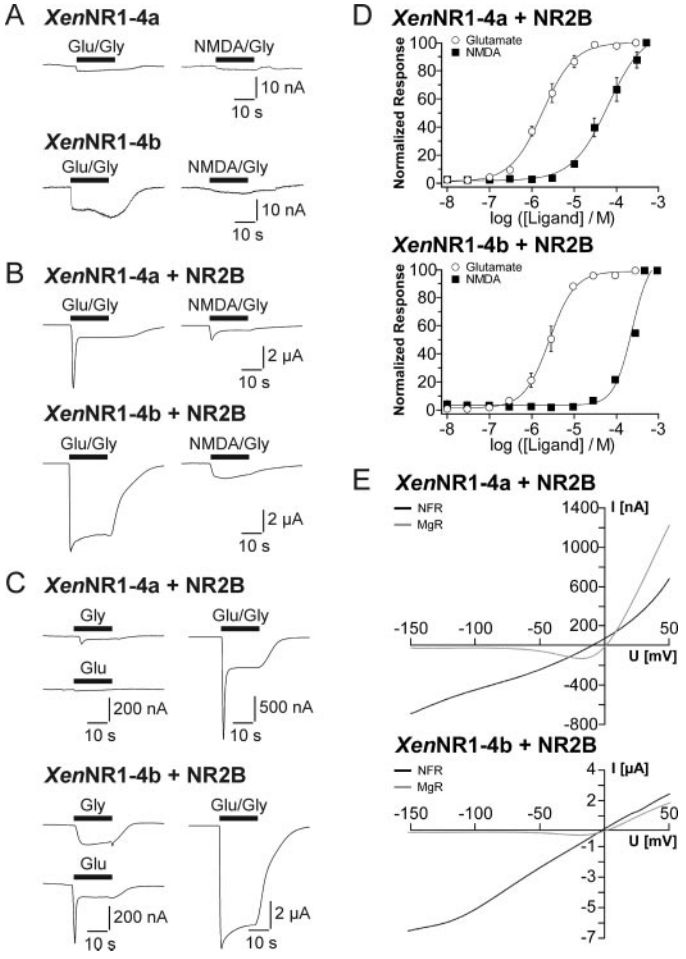

Fig. 2. Properties of currents recorded from *X. laevis* oocytes injected with combinations of receptor subunit cRNAs. Experimental details are described under *Materials and Methods*. Glu, 100 μM glutamate; NMDA, 100 μM NMDA; Gly, 10 μM glycine, unless stated differently. Coapplication of agonists is indicated by black bars. A, representative recordings from oocytes injected with *Xen*NR1-4a (top trace) or *Xen*NR1-4b (bottom trace) cRNAs. B, representative recordings from voltage-clamped oocytes injected with rat NR2B and *Xen*NR1-4a (top trace) or *Xen*NR1-4b (bottom trace) cRNAs. C, representative recordings from oocytes injected with *Xen*NR1-4a plus NR2B (top trace) or *Xen*NR1-4b plus NR2B (bottom trace) cRNAs showing the glycine dependence of glutamate-induced currents. D, glutamate and NMDA dose-response curves determined from oocytes injected with NR2B and *Xen*NR1-4a (top graph) or *Xen*NR1-4b cRNAs (bottom graph). Glutamate (○) and NMDA (■) concentrations were varied whereas the coagonist concentration was maintained at 10 μM glycine. Values are the means ± S.E.M. of four experiments, normalized to the responses to 100 μM glutamate/10 μM glycine or 1 mM NMDA/10 μM glycine. The EC_{50} values are given in the text. E, I/V curves recorded from oocytes injected with rat NR2B and *Xen*NR1-4a (top graph) or *Xen*NR1-4b (bottom graph) cRNAs. Recordings of all cells were done either in Mg^{2+}-free NFR (black curves) or in Mg^{2+}-Ringer's solution (gray curves). Note absence of outward rectification in Mg^{2+}-free NFR.

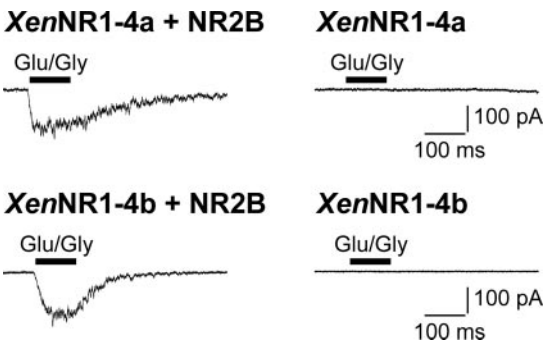

Fig. 3. Representative current traces from patch-clamped HEK293 cells transfected with *X. laevis* NR1 splice variants alone and together with rat NR2B. The application of agonists (100 μM glutamate with 10 μM glycine) is indicated by black bars.

was also shown above for rat NMDA receptor subunits with and without *Xen*U1. Glutamate/glycine induced larger currents (19.2 ± 4.6 nA; $n = 9$) that however, showed no significant difference in their amplitudes compared with the currents recorded in oocytes expressing *Xen*NR1-4b alone (17.9 ± 3.1 nA; $n = 7$; Table 2).

However, as mentioned above, our *Xen*NR1-4b showed a one-amino acid difference in the N-terminal domain compared with the *Xen*NR1-4b of Soloviev et al. (1996). Because we cannot rule out that this minor difference has an effect on the receptor properties, we constructed Soloviev's *Xen*NR1-4b(E166G) cDNA by PCR-mediated mutagenesis (for details, see *Materials and Methods*). This subunit was expressed alone and together with *Xen*U1 in *X. laevis* oocytes to test for pharmacological properties that might indicate the existence of a unitary glutamate receptor. Whereas *Xen*NR1-4b(E166G) forms perfectly functional glutamate/glycine-activated ion channels in oocytes, we could not find any of the unique unitary glutamate receptor properties. As observed for our original *Xen*NR1-4b subunit, kainate or AMPA applied alone never elicited current response. Coapplication of any of those agonists together with glycine in some oocytes yielded tiny currents (1.0–1.8 nA), which in every case were equal in size to currents induced by glycine applied alone (Table 2). Therefore, we interpret these small responses to represent pure glycine currents, as has been shown for all other NMDA receptor subunits investigated. Thus, the single amino acid deviation at position 166 of the mature *Xen*NR1-4b protein does not seem to alter the ion channel properties.

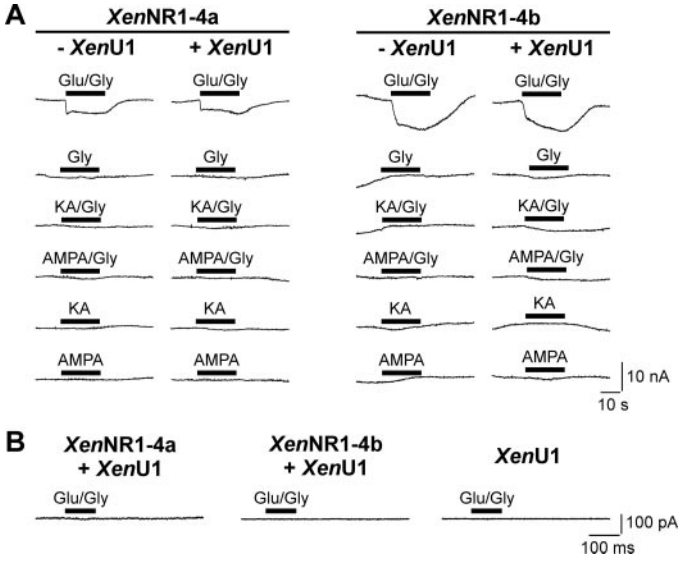

Fig. 4. Pharmacology of the putative unitary glutamate receptor in *X. laevis* oocytes and HEK293 cells. Applied agonist concentrations: Glu, 100 μM glutamate; KA, 100 μM kainate; AMPA, 100 μM AMPA; and Gly, 10 μM glycine. The application of agonists is indicated by black bars. A, comparison of agonist-induced current responses recorded from voltage-clamped oocytes injected with cRNAs of *X. laevis* NR1 splice variants *Xen*NR1-4a and *Xen*NR1-4b alone and together with *Xen*U1. B, representative current responses from patch-clamped HEK293 cells transfected with either *Xen*U1 alone or together with one of the two *X. laevis* NR1-4 splice variants.

Because we could not detect any of the unique non-NMDA receptor agonist-induced currents that were reported to be characteristic for the unitary glutamate receptor, we tried to find other hints for its existence. However, the lack of AMPA-induced currents minimized our chances to re-examine functional properties described by Soloviev et al. (1996). Two characteristics could still be tested: the reported inhibitory effects of 6,7-dinitroquinoxaline-2,3-dione (DNQX) and AMPA. We found that currents induced by coapplication of glutamate (100 μM) and glycine (10 μM) surprisingly were slightly inhibited by coapplied AMPA (100 μM). However, this effect was entirely independent of coexpressed *Xen*U1. Thus, the glutamate/glycine-induced currents were reduced to 70 ± 3% ($n = 5$) and 81 ± 6% ($n = 5$) for *Xen*NR1-4a and *Xen*NR1-4a plus *Xen*U1, respectively. Likewise, we found the currents of *Xen*NR1-4b and *Xen*NR1-4b plus *Xen*U1 to be reduced by coapplication of AMPA to 81 ± 5% ($n = 5$) and 72 ± 6% ($n = 5$), respectively. To test whether this inhibitory effect by AMPA is dependent on the coexpressed *Xen*U1, we coexpressed the *Xen*NR1 subunits with rat NR2B. In this experiment, we also found an AMPA inhibition, to 59 ± 4% ($n = 5$) and 28 ± 7% ($n = 4$) for *Xen*NR1-4a/NR2B and *Xen*NR1-4b/NR2B, respectively. Likewise, an inhibitory effect of DNQX (50 μM) on currents induced by application of NMDA (500 μM) plus glycine (10 μM) was observed. Currents of oocytes expressing any *Xen*NR1-4 splice variant, with or without *Xen*U1, were significantly decreased when DNQX was coapplied (*Xen*NR1-4a, 49 ± 7%, $n = 5$; *Xen*NR1-4a + *Xen*U1, 54 ± 4%, $n = 5$; *Xen*NR1-4b, 63 ± 7%, $n = 5$; and *Xen*NR1-4b + *Xen*U1, 62 ± 7%, $n = 5$). As for AMPA, this effect was also observed in oocytes expressing heteromeric NMDA receptor complexes (*Xen*NR1-4a/NR2B,

TABLE 2

Steady-state currents of *X. laevis* NR1-4 splice variants alone and together with *Xen*U1

The currents given are the means ± S.E.M. The numbers of oocytes measured are given in parentheses. Note that currents smaller than 1 nA are not detectable in the *X. laevis* oocyte expression system. Values smaller than 1 nA result from averaging cells showing currents ≥1 nA with cells showing no current response upon application of the same agonist(s). *Xen*NR1-4b(E166G) has the exact same amino acid sequence as the clone used by Soloviev et al. (1996).

Expressed Subunit	Steady-State Current					
	Glu/Gly (100 μM/10 μM)	KA/Gly (100 μM/10 μM)	AMPA/Gly (100 μM/10 μM)	Gly (10 μM)	KA (100 μM)	AMPA (100 μM)
	nA					
*Xen*NR1-4a						
+ *Xen*U1	3.8 ± 0.3 (7)	0 (6)	0 (6)	0 (6)	0 (6)	0 (6)
− *Xen*U1	4.2 ± 0.9 (7)	0 (6)	0 (6)	0 (6)	0 (6)	0 (6)
*Xen*NR1-4b						
+ *Xen*U1	19.2 ± 4.6 (9)	0.3 ± 0.3 (5)	0.3 ± 0.3 (5)	0.2 ± 0.2 (5)	0 (5)	0 (5)
− *Xen*U1	17.9 ± 3.1 (7)	0 (6)	0 (6)	0 (6)	0 (6)	0 (6)
*Xen*NR1-4b (E166G)						
+ *Xen*U1	50.1 ± 6.0 (6)	0.7 ± 0.3 (6)	0.4 ± 0.2 (6)	0.3 ± 0.2 (6)	0 (6)	0 (6)
− *Xen*U1	49.5 ± 12.4 (6)	0.2 ± 0.2 (5)	0.5 ± 0.3 (5)	0.7 ± 0.3 (6)	0 (5)	0 (5)

32 ± 2%, $n = 5$; and *Xen*NR1-4b/NR2B, 33 ± 8%, $n = 4$). Therefore, the inhibitory effects of DNQX and AMPA do not seem to be unique unitary glutamate receptor properties as postulated (Soloviev et al., 1996) but rather are a normal feature of *X. laevis* NMDA receptors.

Because we did not find any of the reported unique unitary glutamate receptor properties in oocytes, we turned to investigating the existence of this unique receptor type in a mammalian cell line that unlike *X. laevis* oocytes does not express *Xen*U1 endogenously. We expressed *Xen*NR1-4a as well as *Xen*NR1-4b and *Xen*NR1-4b(E166G) together with *Xen*U1 in HEK293 cells. To rule out that *Xen*U1 generates functional homomeric receptor complexes in HEK293 cells, we also expressed *Xen*U1 alone. However, we never obtained significant current on any cell analyzed, regardless whether it expressed *Xen*U1 alone ($n = 13$; Fig. 4B) or *Xen*NR1-4a/*Xen*U1 ($n = 30$), *Xen*NR1-4b/*Xen*U1 ($n = 34$). Because Soloviev et al. (1996) based all their evidence for the existence of a unitary glutamate receptor on patch-clamp experiments in HEK293 cells, we additionally investigated electrophysiologically the *Xen*NR1-4b(E166G)/*Xen*U1 subunit combination in HEK293 cells. In none of the cells tested ($n = 12$) did we get a current response upon application of glutamate/glycine, although *Xen*NR1-4b(E166G) forms functional ion channels in coexpression with rat NR2B (data not shown). Because the lack of current response may have been due to a lack of expression of *Xen*U1 protein, expression was tested by Western blot analysis. Because there is no commercially available antibody against *Xen*U1, we C-terminally tagged the protein with a myc-/polyhistidine-tag (for details, see *Materials and Methods*). The cDNA encoding *Xen*U1-myc-His was transfected into HEK293 cells and 40 h after transfection, we performed a membrane preparation. Membrane proteins were solubilized and separated by SDS-polyacrylamide gel electrophoresis, blotted onto a nitrocellulose membrane, and the presence of *Xen*U1-myc-His was checked using a mouse anti-myc antibody. This experiment confirmed that *Xen*U1-myc-His is expressed in HEK293 cells (Fig. 5). Although lack of *Xen*U1 expression was thus ruled out, it was still possible that *Xen*U1 was not located in the plasma membrane and therefore was unable to interact with *Xen*NR1 to form a unitary glutamate receptor. We therefore investigated the intracellular localization of the *X. laevis* glutamate receptor subunits by means of confocal microscopy. We C-terminally tagged *Xen*U1 with DsRed2 and the two *Xen*NR1-4 splice variants with EGFP. cDNAs encoding these fusion proteins were transfected into HEK293 cells either separately or in combinations: *Xen*NR1-4a-EGFP, *Xen*NR1-4b-EGFP, *Xen*U1-DsRed2, *Xen*NR1-4a-EGFP plus *Xen*U1-DsRed2, and *Xen*NR1-4b-EGFP plus *Xen*U1-DsRed2 (Fig. 6). We found that *Xen*U1-DsRed2 was strongly expressed in the plasma membrane. When we expressed the EGFP-tagged *X. laevis* NR1-4 splice variants alone, we found green fluorescence in the plasma membrane as well as inside the cells (Fig. 6A). Upon coexpression of *Xen*NR1 and *Xen*U1, we found that each subunit was localized to the same regions as when it was expressed alone. *Xen*U1 coexpression did not lead to an increase in *Xen*NR1-4 plasma membrane expression or to a reduction in intracellular *Xen*NR1-4 fluorescence (compare Fig. 6, A with B). *Xen*NR1 and *Xen*U1 subunits were colocalized in the plasma membrane (Fig. 6B). Thus, both subunits clearly are in a position to interact to form a heteromeric complex. Nevertheless, as described above, no indication of the unitary glutamate receptor pharmacology could be detected electrophysiologically.

If *Xen*U1 does not interact with NR1 subunits, it is unlikely that *Xen*U1 has the function of an NR2 substitute in *X. laevis* CNS as had been suggested previously (Soloviev and Barnard, 1997). This means that to generate functional NMDA receptors *X. laevis* has to express a functional equivalent to mammalian NR2 subunits. Therefore, we expected *X. laevis* to possess glutamate receptor subunits that are homologous to the rat NR2 subunits. To prove this hypothesis, we screened *X. laevis* brain cDNA for other glutamate receptors than *Xen*NR1, particularly NR2 subunits. This was done by RT-PCR using the same degenerated primers we previously used for generating the *Xen*NR1 probe. The amplified DNA fragments were subcloned and analyzed by sequencing. We identified fragments of *X. laevis* glutamate receptor subunits that were homologous to rat GluR1 (=*Xen*GluR1; 489 bp), GluR2 (=*Xen*GluR2; 492 bp), and NR2B (=*Xen*NR2B; 480 bp). Compared with its rat homolog

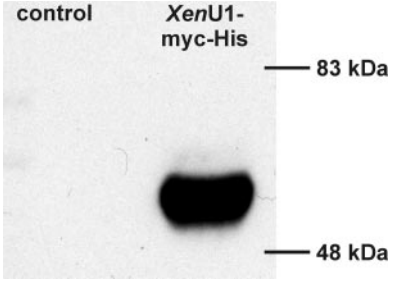

Fig. 5. Western blot analysis of a crude membrane preparation (for details, see *Materials and Methods*) of HEK293 cells expressing *Xen*U1-myc-His. For protein detection, a mouse anti-myc antibody was used.

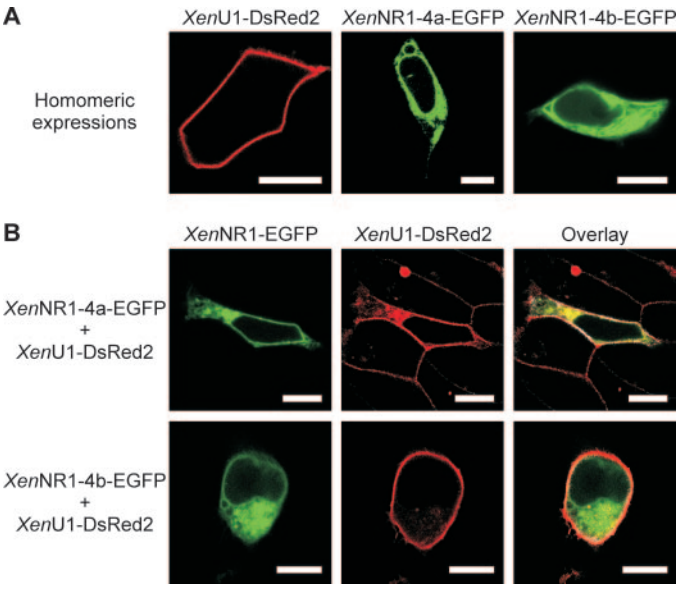

Fig. 6. Subcellular localization of *X. laevis* glutamate receptor subunits in HEK293 cells. The white bars in the right corners of the pictures indicate 10 μm. A, representative laser scanning confocal pictures of HEK293 cells expressing *Xen*U1-DsRed2, *Xen*NR1-4a-EGFP, or *Xen*NR1-4b-EGFP. B, representative laser scanning confocal pictures of HEK293 cells expressing the EGFP-tagged *Xen*NR1 splice variants *Xen*NR1-4a (top) or *Xen*NR1-4b (bottom) together with *Xen*U1-DsRed2. Colocalization is highlighted by white dots in the overlay pictures (right column).

*Xen*NR2B shows 81.7% sequence identity at the nucleotide level (Fig. 7) and 98% at the amino acid level. These data show that *X. laevis* actually possesses NR2 subunits and thus does not require *Xen*U1 as an NR2 substitute. Therefore, *Xen*U1 has to be classified as a *X. laevis* kainate binding protein of unknown function.

Discussion

Coexpression of the *X. laevis* KBP *Xen*U1 with Rat NR1 Splice Variants in *X. laevis* Oocytes Does Not Generate a Unitary Glutamate Receptor. When Green et al. (2002) re-examined the unitary glutamate receptor, they could not confirm its existence, although they used the same methods as Soloviev et al. (1996): ligand binding studies, electrophysiological analysis in HEK293 cells and additionally in *X. laevis* oocytes, and coimmunoprecipitation experiments. However, proponents of the unitary glutamate receptor concept could criticize the study by Green et al. (2002) based on the fact that they used exclusively rat NR1-1a, which is a different NR1 splice variant and originates from a different species compared with the one used in the original reports (Soloviev et al., 1996, 1998). To rule out the existence of any possible splice variant-dependent interaction between NR1 and *Xen*U1, we tested all eight rat NR1 splice variants (Hollmann et al., 1993) in our attempts to re-examine the postulated unitary glutamate receptor. However, none of the

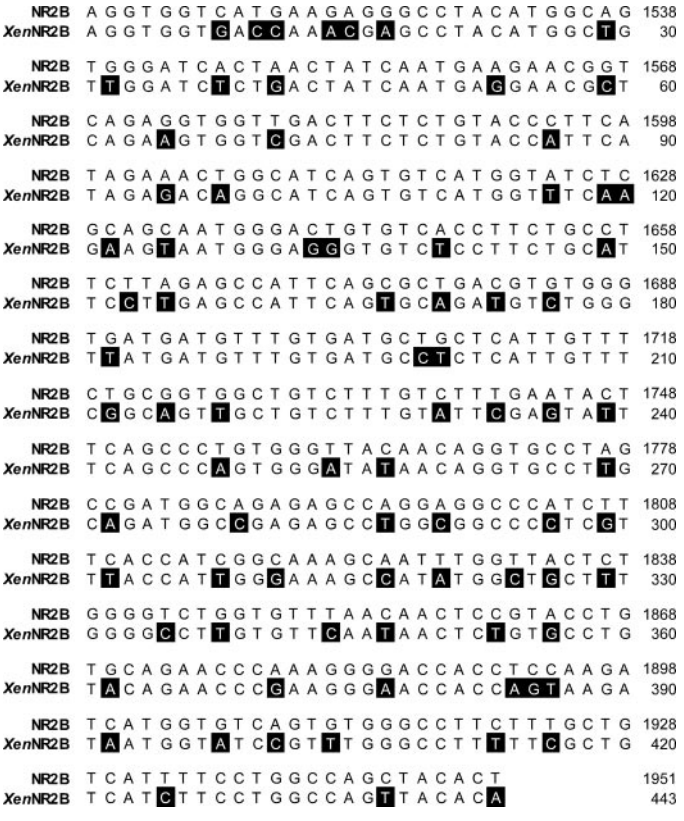

Fig. 7. Sequence alignment of a 443-bp *X. laevis* NR2B (*Xen*NR2B) fragment with rat NR2B cDNA (GenBank accession no. U11419). The numbers given to the right of the sequences indicate the nucleotide positions of the line's last nucleotide in the rat NR2B complete coding region and of the amplified *Xen*NR2B fragment, respectively. Sequence differences of *Xen*NR2B compared with rat NR2B are highlighted with black boxes. Note that the *Xen*NR2B sequence shown does not contain the regions complementary to the degenerated primers used for screening.

splice variants showed a hint of the reported unique unitary glutamate receptor pharmacology. We only confirmed the well-known glutamate/glycine-induced currents and additionally observed tiny currents induced by glycine alone, the latter of which were never observed by Soloviev et al. (1996). Because we used rat NR1 subunits in this splice variant comparison, we could not rule out a possible species-dependent interaction at this point.

Structural, Functional, and Subcellular Localization Analysis of *Xen*NR1-4a and *Xen*NR1-4b with and without *Xen*U1 Fails to Detect Evidence for the Existence of the Unitary Glutamate Receptor. To investigate the exact same subunit combinations from the exact same species as used by Soloviev et al. (1996), we cloned two *X. laevis* NR1 splice variants: *Xen*NR1-4a and *Xen*NR1-4b. These subunits were identical to the published *Xen*NR1 (Soloviev et al., 1996), except for one amino acid in position 166 in the N-terminal domain. The additional construction and electrophysiological investigation of *Xen*NR1-4b(E166G), which is a clone encoding the exact same amino acid sequence as was used by Soloviev et al. (1996), showed that this single-amino acid deviation does not alter any pharmacological properties and did not lead to the formation of a unitary glutamate receptor when coexpressed with *Xen*U1. Contrary to Soloviev et al. (1996), we found the a splice variant to be more abundant in *X. laevis* CNS than the b variant. A similar relationship had previously been shown for mammalian NR1 subunits (Sugihara et al., 1992; Hollmann and Heinemann, 1994). We confirmed the finding of Soloviev et al. (1996) that the N terminus of *Xen*NR1 is 13% different from rat NR1. This sequence difference was suggested to alter the functional properties of the NR1 subunit, thus enabling *Xen*NR1 to interact efficiently with *Xen*U1 (Soloviev et al., 1996). Because a full characterization of *Xen*NR1 has not been reported, we extensively characterized the functional properties of *Xen*NR1-4a and *Xen*NR1-4b. We found no functional differences between the *X. laevis* NR1 subunits and their rat homologs. The *Xen*NR1 splice variants in our hands showed all the properties reported for rat NR1 subunits, such as activation by glutamate/glycine, NMDA/glycine, and glycine alone (Moriyoshi et al., 1991); glycine dependence of the induced currents (Kleckner and Dingledine, 1988; Laube et al., 1993); interaction with NR2 subunits (Ikeda et al., 1992; Kutsuwada et al., 1992; Meguro et al., 1992); similar EC_{50} values; linear I/V curves in the absence of Mg^{2+}; block by extracellular Mg^{2+} ions; and block by MK-801 (Hollmann et al., 1993). In addition, we found two alleged unique unitary glutamate receptor properties (Soloviev et al., 1996) to occur in both *X. laevis* and rat NMDA receptors in the absence of *Xen*U1: although AMPA and DNQX indeed antagonize agonist-induced currents at *Xen*NR1 plus *Xen*U1, the same effect can be demonstrated for *Xen*NR1 expressed alone as well as in coexpression with rat NR2B. We never saw current upon application of non-NMDA receptor agonists in oocytes expressing *Xen*NR1 with or without *Xen*U1. In HEK293 cells, we never detected currents upon application of glutamate/glycine, although the cells were transfected with the same subunit combination, *Xen*NR1-4b plus *Xen*U1, which Soloviev et al. (1996) had used in their studies in HEK293 cells where they had observed currents. We also recorded from cells transfected separately with *Xen*NR1 ($n = 31$) and *Xen*U1 ($n = 13$) as negative controls and never obtained

currents. By contrast, Soloviev et al. (1996) detected in one of 27 and two of 89 cells unexplained currents for "homomeric" *Xen*NR1 and *Xen*U1 receptors, respectively (Soloviev et al., 1996). This is surprising because NR1 subunits expressed homomerically in mammalian cell lines in other studies have not been reported to form functional ion channels (Dingledine et al., 1999). Likewise, it had been reported that *Xen*U1 does not form functional ion channels alone (Ishimaru et al., 1996), a property that is matched by the other five known KBPs (Henley, 1994; Hollmann, 1999). Using confocal microscopy, we showed that the lack of function in our experiments is not caused by a lack of expression. We demonstrated that *Xen*NR1 and *Xen*U1 are expressed in the plasma membrane and thus are in a position to interact to form the postulated unitary glutamate receptor. Therefore, as the subunit combinations *Xen*NR1-4a plus *Xen*U1 and *Xen*NR1-4b plus *Xen*U1 used by Soloviev et al. (1996) fail to generate a unitary glutamate receptor pharmacology despite proven membrane expression of all three subunits and proven functionality of *Xen*NR1-4a and *Xen*NR1-4b, we conclude that NR1 subunits do not form the postulated unitary glutamate receptor upon coexpression with *Xen*U1.

The *X. laevis* KBP *Xen*U1 Does Not Replace NR2 Subunits in the CNS of *X. laevis*. After Soloviev et al. (1996) postulated that *Xen*U1 can interact with NR1 subunits to generate the unitary glutamate receptor, it was suggested that *Xen*U1 may be a substitute for NR2 subunits in *X. laevis* CNS (Soloviev and Barnard, 1997). This hypothesis was supported by PCR-mediated screening experiments for *X. laevis* NR2 subunits, which did not lead to the identification of any such subunits (Soloviev and Barnard, 1997), despite evidence for their existence from the observed crossreactivity of an anti-rat NR2 antibody with *X. laevis* CNS proteins (Soloviev et al., 1996). However, when we used the same strategy as Soloviev and Barnard (1997) in screening experiments to identify an NR2 homolog in *X. laevis* brain, we did identify a fragment of a *X. laevis* NR2B subunit, which we termed *Xen*NR2B. Likewise, in contrast to the report by Soloviev et al. (1996), our screening experiments revealed additional *Xen*NR1 splice variants: a *X. laevis* homolog of the alternatively spliced exon 21 was identified, which proved the existence of *Xen*NR1-3 splice variants. This indicates that *X. laevis* NR1 is likely to have the same gene structure and probably undergoes the same splicing events as known from rat NR1 (Hollmann et al., 1993). In addition, the existence of several other *X. laevis* glutamate receptor subunits has been verified: *Xen*GluR1 and *Xen*GluR2 (both in our laboratory; R. Trippe and M. Hollmann, unpublished observations); *Xen*GluR5, and *Xen*GluR6 (Ishimaru et al., 1996). Thus, it is possible to classify functional *X. laevis* glutamate receptors just like mammalian receptors into AMPA, kainate, and NMDA receptor subfamilies (Hollmann, 1999). *Xen*U1 belongs to the subfamily of the KBPs, known from non-mammalian vertebrates such as fish, birds, and amphibians. This is supported by several distinct properties that *Xen*U1 shares with other KBPs (Henley, 1994), such as the high affinity for kainate and AMPA (Ishimaru et al., 1996; Soloviev et al., 1996), a glutamate receptor-untypical short N terminus (Ishimaru et al., 1996), low sequence homology with other glutamate receptor subunits (Hollmann, 1999), and functional ion pore domains (Villmann et al., 1997), despite the fact that full-length KBPs apparently do not form functional homomeric ion channels. The fact that sequence identity of *Xen*U1 is only 67.9% compared with another amphibian KBP (from *Rana pipiens berlandieri*) is not surprising because the sequence identities of KBPs in general are very low; even the two KBPs known from one species (goldfish) only share 60.9% sequence identity (Wo and Oswald, 1994; Hollmann, 1999). Therefore, the low sequence homology of *Xen*U1 compared with other KBPs is no reason to classify *Xen*U1 differently as postulated in Ishimaru et al. (1996) and Soloviev et al. (1996). In addition, if a unitary glutamate receptor exists, it is very unlikely that *Xen*U1 is involved in its formation because most experiments that provided evidence for such a receptor type were done in the mammalian CNS (Jahr and Stevens, 1987) where no KBPs or *Xen*U1 homologs have ever been identified (Hollmann, 1999). Thus, although the *X. laevis* KBP *Xen*U1 is definitely not involved in the formation of a unitary glutamate receptor, its physiological role still poses an interesting question and remains to be elucidated.

Acknowledgments

We thank Prof. Dr. Bernd-Joachim Benecke for providing the mouse anti-myc antibody, Christina Klein for expert technical help with HEK293 cell culture, and Björn Peters for oocyte preparations.

References

Chen C and Okayama H (1987) High-efficiency transformation of mammalian cells by plasmid DNA. *Mol Cell Biol* **7:**2745–2752.
Dingledine R, Borges K, Bowie D, and Traynelis SF (1999) The glutamate receptor ion channels. *Pharmacol Rev* **51:**7–61.
Green T, Rogers CA, Contractor A, and Heinemann SF (2002) NMDA receptors formed by NR1 in *Xenopus laevis* oocytes do not contain the endogenous subunits *Xen*U1. *Mol Pharmacol* **61:**326–333.
Henley JM (1994) Kainate-binding proteins: phylogeny, structures and possible functions. *Trends Pharmacol Sci* **15:**182–190.
Hollmann M (1999) Structure of ionotropic glutamate receptors, in *Ionotropic Glutamate Receptors in the CNS* (Jonas P and Monyer H eds) pp 3–98, Springer-Verlag, Berlin.
Hollmann M, Boulter J, Maron C, Beasley L, Sullivan J, Pecht G, and Heinemann SF (1993) Zinc potentiates agonist-induced currents at certain splice variants of the NMDA receptor. *Neuron* **10:**943–954.
Hollmann M and Heinemann SF (1994) Cloned glutamate receptors. *Annu Rev Neurosci* **17:**31–108.
Hollmann M, Maron C, and Heinemann SF (1994) N-Glycosylation site tagging suggests a three transmembrane domain topology for the glutamate receptor GluR1. *Neuron* **13:**1331–1343.
Hollmann M, O'Shea-Greenfield MA, Rogers SW, and Heinemann SF (1989) Cloning by functional expression of a member of the glutamate receptor subfamily. *Nature (Lond)* **342:**643–648.
Ikeda K, Nagasawa M, Mori H, Araki K, Sakimura K, Watanabe M, Inoue Y, and Mishina M (1992) Cloning and expression of the e4 subunit of the NMDA receptor channel. *FEBS Lett* **313:**34–38.
Ishii T, Moriyoshi K, Sugihara H, Sakurada K, Kadotani H, Yokoi M, Akazawa C, Shigemoto R, Mizuno N, Masu M, et al. (1993) Molecular characterization of the family of the *N*-methyl-D-aspartate receptor subunits. *J Biol Chem* **268:**2836–2843.
Ishimaru H, Kamboj R, Ambrosini A, Henley JM, Soloviev MM, Sudan H, Rossier J, Abutidze K, Rampersad V, Usherwood PNR, et al. (1996) A unitary non-NMDA receptor short subunit from *Xenopus*: DNA cloning and expression. *Receptors Channels* **4:**31–49.
Jahr CE and Stevens CF (1987) Glutamate activates multiple single channel conductances in hippocampal neurons. *Nature (Lond)* **325:**522–525.
Johnson JW and Ascher P (1987) Glycine potentiates the NMDA response in cultured mouse brain neurons. *Nature (Lond)* **325:**529–531.
Kleckner NW and Dingledine R (1988) Requirement for glycine in activation of NMDA-receptors expressed in *Xenopus* oocytes. *Science (Wash DC)* **241:**835–837.
Kutsuwada T, Kashiwabuchi N, Mori H, Sakimura K, Kushiya E, Araki K, Meguro H, Masaki H, Kumanishi T, Arakawa M, et al. (1992) Molecular diversity of the NMDA receptor channel. *Nature (Lond)* **358:**36–41.
Laube B, Kuryatov A, Kuhse J, and Betz H (1993) Glycine-glutamate interactions at the NMDA receptor: role of cysteine residues. *FEBS Lett* **335:**331–334.
Leonard JP and Kelso SR (1990) Apparent desensitization of NMDA responses in *Xenopus* oocytes involves calcium-dependent chloride current. *Neuron* **4:**53–60.
Mayer ML and Westbrook GL (1987) The physiology of excitatory amino acids in the vertebrate central nervous system. *Prog Neurobiol* **28:**197–276.
Meguro H, Mori H, Araki K, Kushiya E, Kutsuwada T, Yamazaki M, Kumanishi T,

Arakawa M, Sakimura K, and Missina M (1992) Functional characterization of a heteromeric NMDA receptor channel expressed from cloned cDNAs. *Nature (Lond)* **357:**70–74.
Monyer H, Sprengel R, Schoepfer R, Herb A, Higuchi M, Lomeli H, Burnashev N, Sakmann B, and Seeburg PH (1992) Heteromeric NMDA receptors: molecular and functional distinction of subtypes. *Science (Wash DC)* **256:**1217–1221.
Moriyoshi K, Masu M, Ishii T, Shigemoto R, Mizuno N, and Nakanishi S (1991) Molecular cloning and characterization of the rat NMDA receptor. *Nature (Lond)* **354:**31–37.
Soloviev MM, Abutidze K, Mellor I, Streit P, Grishin EV, Usherwood PN, and Barnard EA (1998) Plasticity of agonist binding sites in hetero-oligomers of the unitary glutamate receptor subunit *Xen*U1. *J Neurochem* **71:**991–1001.
Soloviev MM and Barnard EA (1997) *Xenopus* oocytes express a unitary glutamate receptor endogenously. *J Mol Biol* **273:**14–18.
Soloviev MM, Brierley MJ, Shao ZY, Mellor IR, Volkova TM, Kamboj R, Ishimaru H, Sudan H, Harris J, Foldes RL, et al. (1996) Functional expression of a recombinant unitary glutamate receptor from *Xenopus*, which contains *N*-methyl-D-aspartate (NMDA) and non-NMDA receptor subunits. *J Biol Chem* **271:**32572–32579.
Sugihara H, Moriyoshi K, Ishii T, Masu M, and Nakanishi S (1992) Structures and properties of seven isoforms of the NMDA receptor generated by alternative splicing. *Biochem Biophys Res Commun* **185:**826–832.
Udgaonkar JB and Hess GP (1987) Chemical kinetic measurements of a mammalian acetylcholine receptor by fast-reaction technique. *Proc Natl Acad Sci USA* **84:**8758–8762.
Villmann C, Bull L, and Hollmann M (1997) Kainate binding proteins possess functional ion channel domains. *J Neurosci* **17:**7634–7643.
Watkins JC and Evans RH (1981) Excitatory amino acid transmitters. *Annu Rev Pharmacol Toxicol* **21:**165–204.
Wo ZG and Oswald RE (1994) Transmembrane topology of two kainate receptor subunits revealed by N-glycosylation. *Proc Natl Acad Sci USA* **91:**7154–7158.
Wo ZG and Oswald RE (1995) A topological analysis of goldfish kainate receptors predicts three transmembrane segments. *J Biol Chem* **270:**2000–2009.

Address correspondence to: Prof. Dr. M. Hollmann, Department of Biochemistry I-Receptor Biochemistry, Ruhr University Bochum, Universitaetsstrasse 150, Building NC, Level 6, Room 170, D-44789 Bochum, Germany. E-mail: michael.hollmann@rub.de